SOILS AND FOUNDATIONS Vol. 42, No. 1, 1–7, Feb. 2002
Japanese Geotechnical Society

COLLAPSE LOADS OVER TWO-LAYER CLAY FOUNDATION SOILS

RADOSLAW L. MICHALOWSKI[i)]

ABSTRACT

A strict upper bound solution to limit loads on strip footings over two-layer clay foundation soil is presented. Two mechanisms of failure are considered: one with a continually deforming field, and a rigid-block mechanism. The multi-block mechanism was found to be very flexible in terms of being able to assume different shapes of the deformation pattern. Consequently, this mechanism yielded the least upper bound to the bearing pressure. The method used was adapted to calculations of bearing capacity of strip footings subjected to loads with horizontal components. If the depth of the second layer of clay is sufficiently large, the shear strength of this layer will not affect the bearing capacity. This depth is referred to here as the critical depth, and it depends on the footing width and the combination of the undrained shear strength in the two layers. If the undrained shear strength of the bottom layer is small compared to the top layer, the critical height may be as much as twice the footing width.

Key words: bearing capacity, clays, footings, layered soil, limit analysis, shallow foundations (**IGC**: E3)

INTRODUCTION

Considerations of stability of geotechnical structures include a renewed interest in limit analysis. This is due to new applications, such as reinforced soil (Michalowski, 1997), but it is also due to development of numerical techniques in limit analysis, such as that presented by Tamura et al. (1984), or Sloan (1988) and Sloan and Kleeman (1994). Numerical solutions, both lower and upper bounds, were shown recently by Merifield et al. (1999) for the problem of the bearing capacity of a two-layer clay foundation. This problem was considered earlier in the context of limit analysis with a specific application to embankments on soft clay with a strong crust layer (Michalowski, 1992). For some range of parameters, these earlier results yield a better upper bound than that in Merifield et al. (1999). This might lead to the conclusion that the upper bound calculations based on optimization of the mechanism through sequential modification of its geometry (and the geometry of the hodograph) may be less restrictive, in some cases, than the linear programming approach (Merifield et al., 1999). However, the linear programming approach to solving for the lower bounds (Sloan, 1988) appears to be a far more effective tool than the traditional approach of "guessing" the admissible stress distribution.

In addition to theoretical approaches to the bearing capacity of layered foundation soils, there have been attempts to obtain solutions through semi-empirical considerations (Meyerhof and Hanna, 1978). These solutions are difficult to judge as they are based on small-scale tests. At best, they can be considered approximate solutions without a sense of upper or lower bounds.

The first rational approach to solving the bearing capacity problem for a two-layer clay foundation soil was shown by Button (1953). While not indicated at the time, Button's calculations were equivalent to limit analysis based on the kinematic approach. His calculations were later repeated, and generalized for anisotropic clays by Reddy and Srinivasan (1967), and given in the context of limit analysis by Chen (1975). These results are used here as a reference, and are referred to as Chen (1975) solutions.

In addition to symmetric bearing capacity, the limit load on a two-layer foundation clay is calculated for inclined loads. The parameter used to represent the intensity of the horizontal component of the load is selected as a ratio of the average shear stress on the footing-soil interface to the undrained strength of the upper clay layer.

This paper focuses exclusively on the kinematic approach. The problem is briefly described in the next section, followed by the fundamentals of the approach to solving the problem. Both a continuous and a rigid-block mechanism of foundation soil collapse are then discussed, followed by sections on critical depth and horizontal load components. The results of computations are shown in the penultimate section, and the paper is concluded with some final remarks.

[i)] Professor, Dept. Civil and Environmental Engineering, University of Michigan, Ann Arbor, MI 48109-2125; e-mail: rlmich@umich.edu; fax: 734 764-4292.
Manuscript was received for review on May 26, 2000.
Written discussions on this paper should be submitted before September 1, 2002 to the Japanese Geotechnical Society, Sugayama Bldg. 4F, Kanda Awaji-cho 2-23, Chiyoda-ku, Tokyo 101-0063, Japan. Upon request the closing date may be extended one month.

PROBLEM STATEMENT

The solution to be found is to indicate what are the limit loads on a two-layer foundation clay. The limit stress state of clay is described by the Tresca yield condition. The strength parameter in the yield condition is interpreted here as the undrained shear strength of the clay. To simulate this problem, a footing is placed on the surface of a half space whose top layer is characterized by undrained shear strength c_1, and the clay underneath has strength c_2 (Fig. 1(a)). Because the soil surface is horizontal and the material is frictionless and incompressible, the surcharge load on the surface beyond the footing would increase the bearing pressure by a magnitude equal to the surcharge pressure. The footing has width B, and is infinitely long (strip footing). Hence, a plane-strain deformation pattern is expected. The thickness of the top layer of clay is equal to H. Because the model of the soil is independent of the length scale, the solution to the problem is expected to be dependent on dimensionless parameters H/B and c_1/c_2.

APPROACH

Limit loads on footings are calculated here using the upper bound theorem of limit analysis, which can be mathematically represented by the following inequality

$$\int_V \dot{D}(\dot{\varepsilon}_{ij})dV \geq \int_{S_v} T_i v_i dS_v + \int_{S_t} T_i v_i dS_t + \int_V \gamma_i v_i dV \qquad (1)$$

The integral on the left-hand side of inequality (1) represents the rate of work dissipation during an incipient failure of the foundation soil, and the right-hand side includes the work rates of all the external forces. T_i is the stress vector on boundaries S_v and S_t. Vector T_i is unknown (limit load) on S_v, and it is known on S_t (for instance, surcharge pressure). v_i is the velocity vector in the kinematically admissible mechanism, γ_i is the unit weight vector, and V is the volume of the mechanism.

The mathematical form of the theorem in Eq. (1) states that the rate of energy dissipation is not less than the rate of work of external forces in any kinematically admissible failure mechanism. Hence, the inequality in (1) can be used to calculate the upper bound to the force on boundary S_v, if all the other terms in Eq. (1) are known. In the specific case considered here the last two terms on the right-hand side are equal to zero. The last one being zero is a direct consequence of the principle of mass conservation, whereas the second last is zero because there is no surcharge load considered. Notice that the total force on boundary S_v can be calculated only if velocity v_i on this boundary is constant.

Since the rate of work dissipation is larger than or equal to the rate of work by external forces, equating the two sides of inequality (1) leads to a load on S_v that is not smaller than the true limit load (upper bound). This approach is referred to as the kinematic approach of limit analysis, and it is used in this paper to obtain the limit loads on a two-layer clay foundation soil.

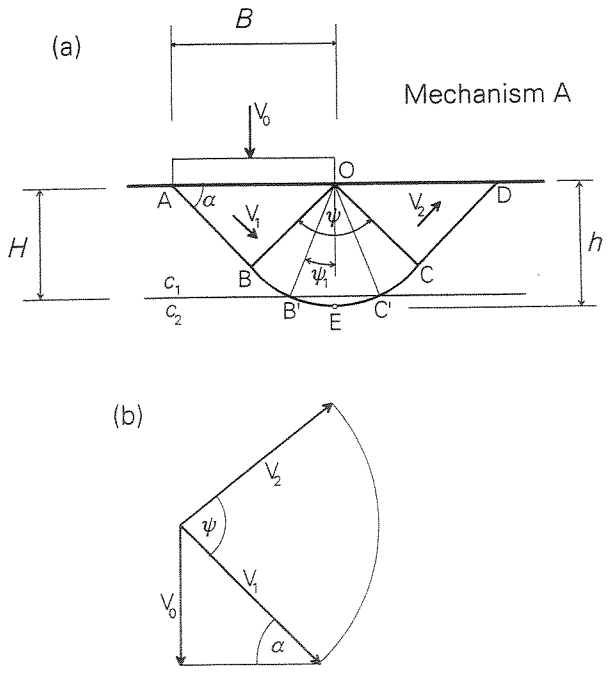

Fig. 1. Collapse pattern (Mechanism A): (a) velocity field, and (b) hodograph

CONTINUOUS DEFORMATION MECHANISMS OF FOUNDATION SOIL COLLAPSE

A failure mechanism most often used in analysis of collapse of a clay foundation is based on the Prandtl solution (Prandtl, 1920) for soil with internal friction angle equal to zero. This solution was adopted by Hill (1950), who modified it for a smooth punch-indentation problem. While the Prandtl result was based on solving hyperbolic-type differential equations for the stress field, this solution also can be arrived at through the kinematic approach of limit analysis. For an ideal vertically loaded surface foundation the two solutions are identical, and they were proven by Shield (1954) to be the exact solutions to the limit load.

The solution by Prandtl cannot be directly used for two-layer foundation soils or for footings loaded with inclined loads. To arrive at rational solutions, a mechanism of failure can be adopted in a form similar to that associated with the Prandtl solution, in which the geometry is allowed to conform to its most adverse shape. This is done through optimization of the collapse mechanism, so that the least upper bound solution is obtained. Such a mechanism is shown in Fig. 1, and it is referred to as Mechanism A.

Line ABCD in Fig. 1(a) is a trace of a velocity discontinuity surface, which, in general, extends through both layers of clay. If this line is smooth at points B and C, then OB and OC are not discontinuities in the velocity field. Blocks ABO and CDO move as rigid bodies, whereas region BCO deforms in a continual manner. The hodograph is shown in Fig. 1(b).

The energy dissipation rate needs to be integrated along line ABCD and within continually deforming region BCO. Depending on the location of points B and C with respect to the interface between the two layers, one can distinguish five different cases. The thickness of the first layer is H. To illustrate the calculations we show the case where both B and C are within the top layer of clay.

The velocity boundary condition is the vertical component of the footing velocity v_0. Since the magnitude of the velocity jump vector along ABCD is constant ($v_0/\sin\alpha$, *see* hodograph), the dissipation rate due to shear along this line is equal to

$$\dot{D}_1=\frac{v_0}{\sin\alpha}\,[c_1(AB+BB'+C'C+CD)+c_2B'C'] \tag{2}$$

The work dissipation rate per unit volume within region BCO is

$$\dot{d}=(\dot{\varepsilon}_1-\dot{\varepsilon}_3)c \tag{3}$$

where $\dot{\varepsilon}_1$ and $\dot{\varepsilon}_3$ are the major and minor principal strain rates, respectively. The strain rates expressed in the polar coordinate system are (r and θ are the polar coordinates with point O being the origin of the system)

$$\dot{\varepsilon}_{rr}=-\frac{\partial v_r}{\partial r}=0$$

$$\dot{\varepsilon}_{\theta\theta}=-\frac{1}{r}\frac{\partial v_\theta}{\partial\theta}-\frac{v_r}{r}=0$$

$$\dot{\varepsilon}_{r\theta}=-\frac{1}{2}\left(\frac{1}{2}\frac{\partial v_r}{\partial\theta}+\frac{\partial v_\theta}{\partial r}-\frac{v_\theta}{r}\right)=\frac{1}{2r}\frac{v_0}{\sin\alpha}=0 \tag{4}$$

Transforming strain rates in Eq. (4) into the principal rates, and using Eq. (3), the dissipation rate per unit volume in BCO becomes

$$\dot{d}=\frac{c}{r}\frac{v_0}{\sin\alpha} \tag{5}$$

This rate now needs to be integrated separately for regions above and below the interface between the two clay layers. It was found more convenient to perform this integration by first calculating the dissipation rate for the entire region BCO as if it was homogeneous with cohesion equal to c_1, and then subtracting dissipation due to the difference in the undrained strength (c_1-c_2) in region B′EC′B′

$$\dot{D}_2=c_1\frac{v_0}{\sin\alpha}\,\overline{OB}\psi-2\frac{v_0}{\sin\alpha}(c_1-c_2)\times\left\{\overline{OB}\psi_1-H\ln\left[\tan\left(\frac{\pi}{4}+\frac{\psi_1}{2}\right)\right]\right\} \tag{6}$$

where ψ_1 is the angle indicated in Fig. 1

$$\psi_1=\arccos\frac{H}{OB} \tag{7}$$

Now, combining the dissipation rates in Eq. (2) and Eq. (6), and equating them to the rate of work of the external force on the footing

$$\dot{W}_q=\bar{q}Bv_0 \tag{8}$$

leads to the upper bound on the magnitude of the average bearing pressure $\bar{q}$ under the footing

$$\bar{q}=\frac{\dot{D}_1+\dot{D}_2}{Bv_0} \tag{9}$$

Angles α and ψ were varied in an optimization process in order to obtain the least upper bound to bearing pressure $\bar{q}$. Since the depth of the mechanism is not known a priori, other cases were considered where points B and C might be in the bottom layer, B in the top and C in the bottom, etc. The case which yields the minimum of bearing pressure was then taken as the least upper bound for Mechanism A.

RIGID BLOCK MECHANISM

The second mechanism used here consists of rigid blocks separated by velocity discontinuity surfaces, as presented in Fig. 2(a). This mechanism will be referred to as Mechanism B, or as a multi-block mechanism. It resembles the mechanism used earlier by Michalowski and Shi (1995) for calculating the bearing capacity of footings on a sand-clay foundation soil. Although it may seem that this mechanism is less sophisticated than that in Fig. 1, it is expected to yield results as good as or better than those based on Mechanism A, because it is less restrictive in being able to assume different shapes. Segment BC of the discontinuity in Fig. 1(a) is set to be a sector of a circular arc, while line BC in Fig. 2(a) can assume any shape consistent with an incompressible deformation process. Therefore, with a sufficient number of blocks, this mechanism is expected to yield a better

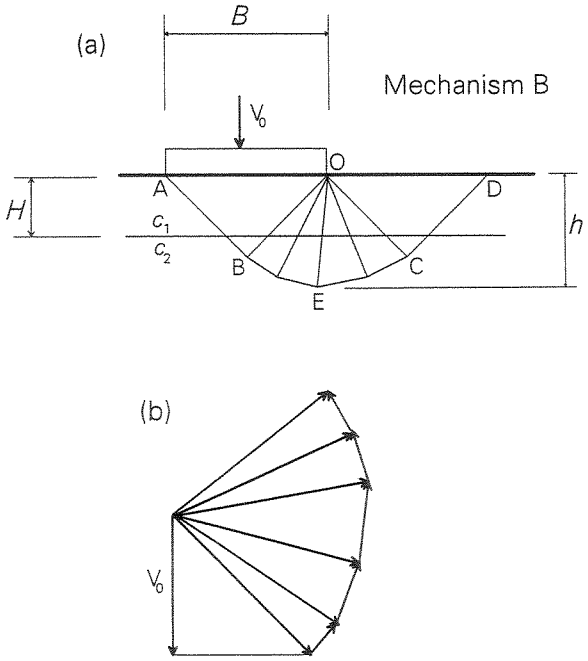

Fig. 2. Multi-block collapse pattern (Mechanism B): (a) velocity field, and (b) hodograph

upper bound than Mechanism A does. The sufficient number of blocks was found to be about 10. For instance, for a case where the thickness of the top layer is 1/4 of the footing width ($H/B=0.25$), and the ratio of the cohesion in the two layers is $c_1/c_2=4$, mechanism B with 10 blocks yields $q/c_1=2.153$, whereas the same mechanism with 50 blocks gives $q/c_1=2.149$ (a difference of less than 0.5%). The energy balance equation for Mechanism B can be easily written down after the work dissipation rate is integrated on all the straight-line velocity discontinuity surfaces, with the velocities being determined from the hodograph (Fig. 2(b)). In calculations, each of the discontinuities intersecting the interface between the two layers was divided into two segments, and the work dissipation was calculated separately for the segments within the top and bottom layers.

HORIZONTAL LOAD COMPONENT

Calculations have been performed for both the vertical and inclined loads. The horizontal component is typically included in considerations as an inclination of the load. While this is appropriate for footings on frictional soils, a more convenient way to describe the horizontal load component on clays is to present its intensity as a fraction of the clay undrained shear strength. Coefficient χ is defined here as the ratio of the intensity of the horizontal load (average shear stress $\bar{\tau}$ on the clay-footing interface) to the undrained shear strength of the soil immediately below the footing

$$\chi=\frac{\bar{\tau}}{c_1} \tag{10}$$

Coefficient χ can vary between 0 (vertical load) to 1 (surface sliding). In general, the depth of the collapse mechanism decreases with an increase in coefficient χ.

RESULTS

Calculations have been carried out using mechanisms A and B. The geometry of both mechanisms was varied so that the lowest limit load was obtained for both collapse modes. In searching for the minimum load associated with Mechanism A, angles α and ψ were varied. The geometry of Mechanism B is less restrictive than that of Mechanism A, but the number of variable parameters is much larger. The multi-block Mechanism B (Fig. 2) consists of triangular blocks, and the geometry of each triangle is determined by two angles. Since the sum of all angles at point O must be equal to π, the number of variables in the optimization process of Mechanism B was $2n-1$, where n is the number of blocks. The number of blocks used in computations was $n=50$ (although when the number of blocks exceeds 10, the bearing pressure changes very little with an increase in n). Out of the two failure loads obtained (for mechanisms A and B), the least upper bound is presented in Tables 1 and 2. The multi-block Mechanism B was more effective than Mechanism A was (it yielded the least upper bound), and

Table 1. Bearing capacity results

H/B	c_1/c_2	q/c_1				Chen 1975	Merifield 1999
		$\chi=0$	$\chi=0.25$	$\chi=0.50$	$\chi=0.75$	$\chi=0$	$\chi=0$
0.125	5	1.520	1.353	1.075	0.631	1.527	1.55
	4	1.766	1.587	1.300	0.852	1.786	1.82
	3	2.166	1.968	1.668	1.213	2.212	2.27
	2	2.933	2.709	2.387	1.916	3.050	3.09
	1.5	3.681	3.436	3.093	2.605	3.878	3.93
	1	5.141	4.857	4.484	3.966	5.520	5.32
	0.8	6.217	5.910	5.514	4.977	6.745	6.36
	0.5	9.391	8.309	6.574	4.758	10.410	8.55
	0.2	9.842	8.309	6.574	4.758	25.015	8.55
0.25	5	1.906	1.790	1.617	1.373	1.900	1.85
	4	2.149	2.021	1.835	1.579	2.153	2.12
	3	2.533	2.389	2.180	1.903	2.559	2.56
	2	3.246	3.090	2.861	2.506	3.334	3.34
	1.5	3.912	3.735	3.417	3.049	4.079	4.08
	1	5.141	4.857	4.484	3.954	5.520	5.32
	0.8	5.991	5.707	4.943	4.037	6.571	6.25
	0.5	6.561	5.879	4.984	4.037	7.973	6.25
	0.2	6.561	5.879	4.984	4.037	7.973	6.25
0.50	5	2.579	2.502	2.394	2.252	2.592	2.44
	4	2.817	2.729	2.610	2.456	2.839	2.74
	3	3.177	3.072	2.934	2.761	3.218	3.16
	2	3.800	3.662	3.488	3.271	3.899	3.89
	1.5	4.329	4.162	3.937	3.675	4.504	4.48
	1	5.141	4.857	4.484	3.954	5.520	5.32
	0.8	5.313	4.903	4.484	3.954	5.697	5.49
	0.5	5.313	4.903	4.484	3.954	5.697	5.49
	0.2	5.313	4.903	4.484	3.954	5.697	5.49

Table 2. Bearing capacity results

H/B	c_1/c_2	q/c_1				Chen 1975	Merifield 1999
		$\chi=0$	$\chi=0.25$	$\chi=0.50$	$\chi=0.75$	$\chi=0$	$\chi=0$
0.75	5	3.190	3.131	3.049	2.947	3.252	2.98
	4	3.420	3.352	3.260	3.146	3.497	3.28
	3	3.756	3.672	3.565	3.433	3.862	3.72
	2	4.299	4.184	4.043	3.873	4.479	4.37
	1.5	4.708	4.558	4.375	3.954	4.977	4.94
	1	5.141	4.857	4.484	3.954	5.520	5.32
	0.8	5.141	4.857	4.484	3.954	5.520	5.36
1.00	5	3.768	3.718	3.652	3.569	3.899	3.54
	4	3.988	3.930	3.856	3.763	4.146	3.83
	3	4.299	4.228	4.138	3.954	4.506	4.24
	2	4.746	4.651	4.484	3.954	5.084	4.82
	1.5	5.046	4.857	4.484	3.954	5.514	5.18
	1	5.141	4.857	4.484	3.954	5.520	5.32
	0.8	5.141	4.857	4.484	3.954	5.520	5.30
1.25	5	4.295	4.280	4.224	3.954	4.540	
	4	4.497	4.482	4.418	3.954	4.792	
	3	4.767	4.715	4.484	3.954	5.153	
	2	5.141	4.857	4.484	3.954	5.520	
	1.5	5.141	4.857	4.484	3.954	5.520	
1.50	5	4.863	4.752	4.484	3.954	5.178	4.56
	4	4.965	4.857	4.484	3.954	5.438	4.84
	3	5.187	4.857	4.484	3.954	5.520	5.15
	2	5.141	4.857	4.484	3.954	5.520	5.31
	1.5	5.141	4.867	4.484	3.954	5.520	5.31

the numbers in Tables 1 and 2 are based on Mechanism B. For a case where $H/B=0.25$ and $c_1/c_2=4$, Mechanism A yields $q/c_1=2.339$ compared to 2.149 for a 50-block Mechanism B (a difference of almost 9%). However the difference between the two results decreases once ratio c_1/c_2 approaches 1, and the two results become identical for homogeneous clay ($c_1/c_2=1$).

The results are given in Tables 1 and 2 in the form of a ratio of the average bearing pressure to the undrained shear strength of the top layer of clay (q/c_1), for different ratios of the undrained shear strength in the two layers (c_1/c_2) and different thickness of the top layer (H/B). In addition to vertically loaded footings, the bearing pressure is given for magnitudes of coefficient χ (*see* Eq. (10)) equal to 0.25, 0.50 and 0.75. For reasons of comparison, the solution to the upper bound by Merifield et al. (1999) is given in the last column. The results from a solution first suggested by Button (1953), and later used by Reddy and Srinivasan (1967) and Chen (1975), are given in the second last column. Both of these solutions are for vertical limit loads only.

The solution suggested in this paper yields a bearing capacity which is always better (lower) than that in the solution by Chen (1975). The solution presented here and the one in Merifield et al. (1999) are close to one another, with one being better for some range of parameters, and the other for other parameters. The approach presented in this paper has some advantages in that the computational effort is relatively low (less than 15 sec. for an optimization of a 50-block mechanism on a 400 MHz Penthium PC). However, the linear programming approach has unquestionable advantages in the lower-bound approach (not discussed here), since it is the only effective method for constructing statically admissible stress fields in the plastic domain and beyond.

For a small thickness of the top layer of clay ($H/B=0.125$) and $c_1>c_2$, the solution by Merifield et al. (1999) yields a result which is not only not as good as the one based on Mechanism B, but it is also not as good as that in Chen (1975). This is surprising, since the latter is based on a crude mechanism, whereas that in Merifield et al. (1999) is based on a rather sophisticated approach.

The bearing pressure decreases substantially with an increase in the horizontal component of the load, which is illustrated in columns 4 to 6 in Table 1 and Table 2. The bearing pressure in these tables can be used for design of footings over two-layer foundations soils.

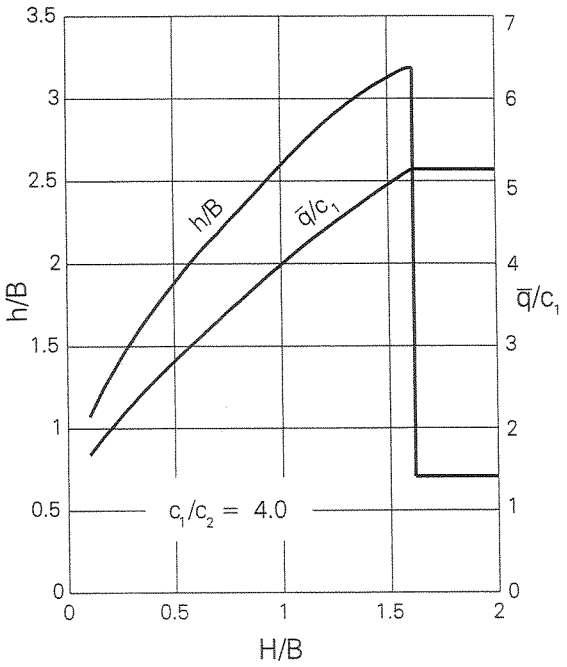

Fig. 3. Depth of the collapse mechanism and bearing pressure as functions of the thickness of the top layer of clay

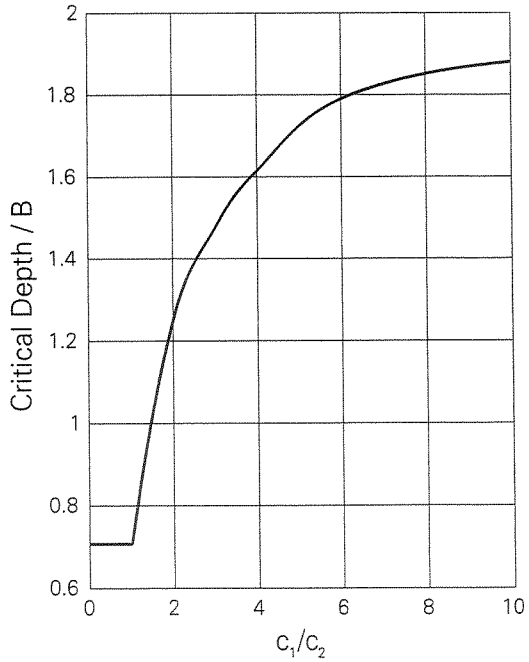

Fig. 4. Critical depth as function of the undrained shear strength ratio

CRITICAL DEPTH

For any combination of the clay strength in the top and bottom layers, there is a depth beyond which the properties of the bottom layer do not affect the bearing capacity. This depth is referred to here as the *critical depth*. Depth h of the collapse mechanism [depth of point E in Fig. 1(a) and Fig. 2(a)] is shown in Fig. 3 as a function of thickness H of the first layer. This graph is for a specific ratio of c_1/c_2 equal to 4.0. The bottom layer is weaker, and, with an increase in the thickness of the first layer (H), the depth of the most adverse mechanism (h) also increases. It seems that the weak soil "attracts" the failure mechanism. The larger the ratio c_1/c_2, the greater the depth to which the mechanism can be attracted. The depth of the most adverse mechanism (mechanism which yields the least upper bound) becomes the greatest [$(h/B)_{max}\approx 3.15$ in this example] when the depth of the weak layer reaches its critical value (here: $H/B\approx 1.6$). When the depth of the bottom layer increases beyond the critical

value, the depth of the mechanism drops down to 0.707, and the mechanism is limited to the top layer only. The bearing pressure increases with an increase in H/B, and it reaches a constant value ($q/c_1 = 5.14$) at the critical depth.

Information about the critical depth for a given c_1/c_2 is useful for practical purposes. Hence, the critical depth is shown in Fig. 4, as a function of undrained strength ratio c_1/c_2. It is evident from this graph that when the bottom layer of clay is considerably weaker than the top clay, e.g., $c_1/c_2 = 10$, the critical depth is almost twice the footing width. However, the depth of the mechanism reaches very deeply into the weak layer. Calculations for $c_1/c_2 = 10$ and the depth of the weak layer of $H = 1.8B$ (B is the footing width) reveal that the depth of the mechanism is almost six times the footing width ($h/B = 5.96$). The bearing pressure in this case was $\bar{q}/c_1 = 4.819$, whereas the much shallower mechanism contained within the top (stronger) layer yields $\bar{q}/c_1 = 5.14$.

SPECIAL CASE

If the bottom layer of clay is much stronger than the top layer, the mechanism may be restricted to the top clay only, and the problem will reduce to the bearing capacity of a layer over a rigid base. While this was a subject of an earlier research (Michalowski, 1992), it is of some interest to indicate that a rigorous upper bound to the bearing pressure can be obtained in a closed form. Although Mechanism B was found to be more effective (it yields limit loads lower than Mechanism A does), computations based on Mechanism B are inherently numerical in nature. Therefore, since the objective of this section is to present a closed-form solution, considerations are limited here to Mechanism A.

In this special case, Mechanism A is considered not to reach into the bottom layer of the foundation soil (Fig. 5). The work dissipation rate for the mechanism in Fig. 5(a) is

$$\dot{D} = \frac{v_0}{\sin\alpha}\left[B\cos\alpha + 2B\psi\sin\alpha + B\sin\alpha\cot(\psi-\alpha)\right]c_1 \tag{11}$$

Considering loading of the footing with the intensity of the horizontal component expressed in Eq. (10), the rate of work of the external forces can be written as

$$\dot{W}_q = Bv_0(\bar{q} + \chi c_1\cot\alpha) \tag{12}$$

By equating Eq. (12) to (11) one arrives at the following expression for the average bearing pressure

$$\frac{\bar{q}}{c_1} = 2\psi + (1-\chi)\cot\alpha + \cot(\psi-\alpha) \tag{13}$$

Two unknown parameters in Eq. (13) are α and ψ. The least bearing pressure requires that angle ψ satisfies

$$\frac{\partial}{\partial\psi}\left(\frac{\bar{q}}{c_1}\right) = 0 \tag{14}$$

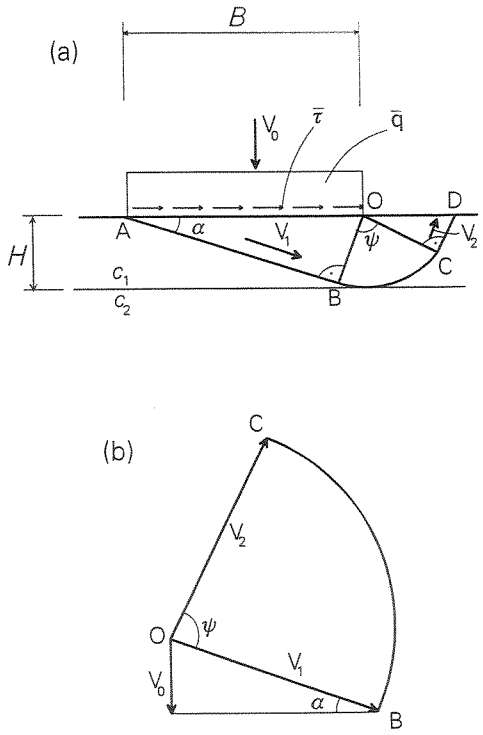

Fig. 5. Collapse within the top layer of clay: (a) failure mechanism, and (b) hodograph

Solving (14) with respect to ψ yields

$$\psi = \frac{\pi}{4} + \alpha \tag{15}$$

and

$$\frac{\bar{q}}{c_1} = 1 + \frac{\pi}{2} + 2\alpha + (1-\chi)\cot\alpha \tag{16}$$

Now, if the top layer of clay is sufficiently thick, condition

$$\frac{\partial}{\partial\alpha}\left(\frac{\bar{q}}{c_1}\right) = 0 \tag{17}$$

determines angle α in the least upper bound solution

$$\alpha = \frac{1}{2}\arccos\chi \tag{18}$$

and the least upper bound becomes

$$\frac{\bar{q}}{c_1} = 1 + \frac{\pi}{2} + \arccos\chi + \sqrt{1-\chi^2} \tag{19}$$

For the solution in Eq. (19) to be valid, the thickness of the top layer (H) must be at least equal to $B\sin\alpha$ (sufficient thickness), where B is the footing width, and α is determined in expression (18). If thickness H is not sufficient, angle α in Eq. (16) reaches its maximum value of

$$\alpha = \arcsin\frac{H}{B} \tag{20}$$

Table 3. Bearing capacity results (special case)

H/B	q/c_1			
	$\chi=0$	$\chi=0.25$	$\chi=0.50$	$\chi=0.75$
0.1	12.721	10.233	7.746	5.258
0.125	10.758	8.774	6.790	4.805
0.2	7.872	6.647	5.427	4.198
0.25	6.949	5.980	5.012	4.044
0.3	6.359	5.565	4.770	3.975
0.4	5.685	5.112	4.539	3.954
0.5	5.350	4.917	4.484	3.954
0.6	5.191	4.857	4.484	3.954
0.7	5.141	4.857	4.484	3.954
0.80	5.141	4.857	4.484	3.954

and

$$\frac{\bar{q}}{c_1}=1+\frac{\pi}{2}+(1-\chi)\sqrt{\left(\frac{B}{H}\right)^2-1}+2\arcsin\frac{H}{B} \quad (21)$$

Computational results based on the solutions in Eq. (19) or Eq. (21) are presented in Table 3. These results are comparable to those in Table 1 for a strong bottom layer ($c_1/c_2=0.2$). For cases with a significant horizontal component of the load, the results in Table 3 are identical to those in Table 1, while for other cases (and $c_1/c_2=0.2$) the bearing pressure from the closed-form solution in Table 3 slightly overestimates that in Table 1.

FINAL REMARKS

A rigorous upper bound solution was presented for the bearing capacity of a two-layer clay foundation soil. The solution is based on the classical approach in which the geometry of the collapse mechanism (and the geometry of the hodograph) is modified in search of the least upper bound. This approach seems to be very effective, and it yields results that, in some regions of parameters, are better (lower) than those produced by the numerical technique based on linear programming (Merifield et al., 1999). Out of the two collapse mechanisms considered, a simple rigid-block pattern was found to be more effective. This is because a large number of rigid blocks allows for the mechanism to assume a variety of different patterns, whereas traditional mechanisms (such as the one attributed to Prandtl) assume the shape of some regions a priori. The approach used is also very economical in terms of computer time.

If the depth of the second layer of clay is sufficiently great, the shear strength of this layer does not affect the bearing capacity. This depth, referred to here as the critical depth, depends on the footing width and the combination of the undrained shear strength in the two layers. If the undrained shear strength of the bottom layer is small compared to the top layer, e.g., $c_1/c_2=10$, the critical height may be as much as twice the footing width. The depth of the mechanism itself, however, can be considerably larger than the critical depth, since the mechanism has a tendency to reach deep into the weak layer (for $c_1/c_2=10$ and $H/B=1.8$, the depth of the mechanism is almost six times the footing width).

The critical depth is an important piece of information in design of footings over layered foundation soils, and it is presented here in the form of a graph.

In addition to the vertical limit load, a solution was obtained to the bearing capacity under inclined loads. The horizontal component of the load makes the collapse mechanism shallower, and it leads to a significant decrease in the bearing capacity.

REFERENCES

1) Button (1953): The bearing capacity of footings on two-layer cohesive subsoil, *Proc. 3rd Int. Conf. SMFE, Zurich*, **1**, 332–335.
2) Chen, W. F. (1975): *Limit Analysis and Soil Plasticity*, Amsterdam: Elsevier.
3) Hill, R. (1950): *Mathematical Theory of Plasticity*, Oxford.
4) Merifield, R. S., Sloan, S. W. and Yu, H. S. (1999): Rigorous plasticity solutions for the bearing capacity of two-layered clays, *Géotechnique*, **49** (4), 471–490.
5) Meyerhof, G. G. and Hanna, A. M. (1978): Ultimate bearing capacity of foundations on layered soils under inclined load. *Can. Geotech. J.*, **15**, 565–572.
6) Michalowski, R. L. (1992): Bearing capacity of nonhomogeneous cohesive soils under embankments, *J. Geotech. Engrg., ASCE*, **118** (7), 1098–1118.
7) Michalowski, R. L. (1997): Stability of uniformly reinforced slopes, *J. Geot. Geoenv. Engrg.*, **123**, 546–556.
8) Michalowski, R. L. and Shi, L. (1995): Bearing capacity of footings over two-layer foundation soils, *J. of Geotech. Eng., ASCE*, **121** (5), 421–428.
9) Prandtl, L. (1920): Über die Härte plastischer Körper, *Nachr. Ges. Wissensch*, Göttingen, math.-phys. Klasse, 74–85.
10) Reddy, A. S. and Srinivasan, R. J. (1967): Bearing capacity of footings on layered clays, *J. Soil Mech. Found. Engrg.*, ASCE, **93** (2), 83–99.
11) Shield, R. T. (1954): Plastic potential theory and Prandtl bearing capacity solution, *J. Appl. Mech., Trans. ASME*, **21**(2), 193–194.
12) Sloan, S. W. (1988): Lower bound limit analysis using finite elements and linear programming, *Int. J. Num. Analyt. Meth. Geomech.*, **12**, 61–67.
13) Sloan, S. W. and Kleeman, P. W. (1994): Upper bound limit analysis using discontinuous velocity fields, *Res. Report No. 096.05.1994*, University of Newcastle, Australia.
14) Tamura, T., Kobayashi, S. and Sumi, T. (1984): Limit analysis of soil structure by rigid plastic finite element method, *Soils and Foundations*, **24** (1), 34–42.